PROCEEDINGS OF SCIENCE

Measurement of CP violation in $\mathrm{B_s} \to \mathrm{J}/\psi\phi$ decays with the CMS experiment

Terhi Järvinen on behalf of the CMS Collaboration*
Helsinki Institute of Physics, University of Helsinki
E-mail: terhi.jarvinen@cern.ch

The CP violating weak phase ϕ_s and the decay width difference $\Delta\Gamma_s$ of the $\mathrm{B_s}$ light and heavy mass eigenstates are measured with the CMS detector at the LHC using a data sample of $\mathrm{B_s} \to J/\psi\phi(1020) \to \mu^+\mu^-\mathrm{K}^+\mathrm{K}^-$ decays. The analysed data correspond to an integrated luminosity of 19.7 fb^{-1} and it is collected in pp collisions at a centre-of-mass energy of 8 TeV. A total of 49 200 reconstructed $\mathrm{B_s}$ candidates are used in the analysis. The weak phase is measured to be $\phi_\mathrm{s} = -0.075 \pm 0.097\ (\mathrm{stat}) \pm 0.031\ (\mathrm{syst})$ rad, and the decay width difference is $\Delta\Gamma_\mathrm{s} = 0.095 \pm 0.013\ (\mathrm{stat}) \pm 0.007\ (\mathrm{syst})\ \mathrm{ps}^{-1}$.

16th International Conference on B-Physics at Frontier Machines
2-6 May 2016
Marseille, France

*Speaker.

PoS(BEAUTY2016)002

1. Introduction

In these proceedings, the measurement [1] of the weak mixing phase ϕ_s of the B_s meson and its decay width difference $\Delta\Gamma_s$ is reported. The data used in the measurement have been collected with the CMS apparatus [2] in run I of the LHC with $\sqrt{s} = 8$ TeV. The data correspond to an integrated luminosity of 19.7 fb^{-1}.

The CP violating weak phase ϕ_s originates from the interference between direct B_s decays into the CP eigenstate $J/\psi\phi$ and the decays via B_s - $\bar{B}_s$ mixing to the same final state. By omitting contributions of penguin processes, the mixing phase is proportional to the angle β_s of a triangle formed using unitary condition of the CKM matrix. More precisely, $\phi_s \simeq -2\beta_s$, where $\beta_s = \arg(-V_{ts}V_{tb}^*/V_{cs}V_{cb}^*)$. The prediction for $2\beta_s = 0.0363^{+0.0016}_{-0.0015}$ rad [3] is determined using a fit to experimental data within the standard model. Because the standard model prediction for ϕ_s is precise, a measurement deviating from the prediction could indicate presence of new particles entering into box diagram of B_s - $\bar{B}_s$ mixing. A prediction for the decay width difference $\Delta\Gamma_s$ in the context of the SM, is $\Delta\Gamma_s = \Gamma_L - \Gamma_H = 0.087 \pm 0.021$ ps^{-1}, where Γ_L and Γ_H are the decay widths of light and heavy B_s mass eigenstates [4]. Previously, the weak mixing phase has been measured at the Tevatron [5] -[8] and later on by ATLAS and LHCb [9]- [14] at the LHC.

To distinguish the CP components of the final state, angular analysis is performed to the decay angles of the B_s decay products. The contribution of the nonresonant $B_s \to J/\psi\, K^+K^-$ channel is taken into account by adding an extra term for this so called S-wave amplitude.

Four dimensional differential decay rate of the B_s meson decaying into $J/\psi\phi$ channel can be modelled as [15]

$$\frac{d^4\Gamma(t)}{d\Theta dt} = f(\Theta,\alpha,t) \propto \sum_{i=1}^{10} O_i(\alpha,t)\cdot g_i(\Theta), \tag{1.1}$$

where O_i are the time-dependent functions, α is a set of physics parameters, Θ represents the decay angles of the B_s meson and g_i are the angular functions presented in transversity basis. The kinematic observables are described using the equations in Table 1.

i	$g_i(\theta_T,\psi_T,\varphi_T)$	N_i	a_i	b_i	c_i	d_i
1	$2\cos^2\psi_T(1-\sin^2\theta_T\cos^2\varphi_T)$	$\lvert A_0(0)\rvert^2$	1	D	C	$-S$
2	$\sin^2\psi_T(1-\sin^2\theta_T\sin^2\varphi_T)$	$\lvert A_\parallel(0)\rvert^2$	1	D	C	$-S$
3	$\sin^2\psi_T\sin^2\theta_T$	$\lvert A_\perp(0)\rvert^2$	1	$-D$	C	S
4	$-\sin^2\psi_T\sin 2\theta_T\sin\varphi_T$	$\lvert A_\parallel(0)\rvert\lvert A_\perp(0)\rvert$	$C\sin(\delta_\perp-\delta_\parallel)$	$S\cos(\delta_\perp-\delta_\parallel)$	$\sin(\delta_\perp-\delta_\parallel)$	$D\cos(\delta_\perp-\delta_\parallel)$
5	$\frac{1}{\sqrt{2}}\sin 2\psi_T\sin^2\theta_T\sin 2\varphi_T$	$\lvert A_0(0)\rvert\lvert A_\parallel(0)\rvert$	$\cos(\delta_\parallel-\delta_0)$	$D\cos(\delta_\parallel-\delta_0)$	$C\cos(\delta_\parallel-\delta_0)$	$-S\cos(\delta_\parallel-\delta_0)$
6	$\frac{1}{\sqrt{2}}\sin 2\psi_T\sin 2\theta_T\sin\varphi_T$	$\lvert A_0(0)\rvert\lvert A_\perp(0)\rvert$	$C\sin(\delta_\perp-\delta_0)$	$S\cos(\delta_\perp-\delta_0)$	$\sin(\delta_\perp-\delta_0)$	$D\cos(\delta_\perp-\delta_0)$
7	$\frac{2}{3}(1-\sin^2\theta_T\cos^2\varphi_T)$	$\lvert A_S(0)\rvert^2$	1	$-D$	C	S
8	$\frac{1}{3}\sqrt{6}\sin\psi_T\sin^2\theta_T\sin 2\varphi_T$	$\lvert A_S(0)\rvert\lvert A_\parallel(0)\rvert$	$C\cos(\delta_\parallel-\delta_S)$	$S\sin(\delta_\parallel-\delta_S)$	$\cos(\delta_\parallel-\delta_S)$	$D\sin(\delta_\parallel-\delta_S)$
9	$\frac{1}{3}\sqrt{6}\sin\psi_T\sin 2\theta_T\cos\varphi_T$	$\lvert A_S(0)\rvert\lvert A_\perp(0)\rvert$	$\sin(\delta_\perp-\delta_S)$	$-D\sin(\delta_\perp-\delta_S)$	$C\sin(\delta_\perp-\delta_S)$	$S\sin(\delta_\perp-\delta_S)$
10	$\frac{4}{3}\sqrt{3}\cos\psi_T(1-\sin^2\theta_T\cos^2\varphi_T)$	$\lvert A_S(0)\rvert\lvert A_0(0)\rvert$	$C\cos(\delta_0-\delta_S)$	$S\sin(\delta_0-\delta_S)$	$\cos(\delta_0-\delta_S)$	$D\sin(\delta_0-\delta_S)$

Table 1: Angular and time-dependent terms of the B_s differential decay rate.

The functions $O_i(\alpha,ct)$ are defined as

$$O_i(\alpha,ct) = N_i e^{-ct/c\tau}\left[a_i\cosh(\frac{1}{2}\Delta\Gamma_s t) + b_i\sinh(\frac{1}{2}\Delta\Gamma_s t) + c_i\cos(\Delta m_s t) + d_i\sin(\Delta m_s t)\right], \tag{1.2}$$

where Δm_s is the mass difference of B_s mass eigenstates and τ is the B_s average lifetime multiplied with speed of light c. The N_i, a_i, b_i, c_i, d_i terms are described in Table 1 and the terms C, S and D

are defined as

$$C = \frac{1-|\lambda|^2}{1+|\lambda|^2}, \qquad S = -\frac{2|\lambda|\sin\phi_s}{1+|\lambda|^2}, \qquad D = -\frac{2|\lambda|\cos\phi_s}{1+|\lambda|^2}, \tag{1.3}$$

using the same sign convention as LHCb. Eq. 1.1 represents the model for B_s and the model for $\bar{B}_s$ is obtained by switching the sign of the c_i and d_i terms. The parameters $|A_\perp|^2$, $|A_0|^2$ and $|A_\parallel|^2$ are the squared magnitudes of the perpendicular, longitudinal, and parallel P-wave amplitudes and the parameters $\delta_\perp$, δ_0, $\delta_\parallel$ are their corresponding strong phases. Amplitude $|A_S|$ represents the nonresonant S-wave amplitude and δ_S is its strong phase.

The CP violating parameters λ_i are defined as $\lambda_i = (q/p)(A_i/\bar{A}_i)$. Amplitudes A_i ($\bar{A}_i$) describe the decay of B_s ($\bar{B}_s$) to the final state i. The parameters p and q weight the flavour states such as $B_H = pB_s^0 - q\overline{B}_s^0$ and $B_L = pB_s^0 + q\overline{B}_s^0$ [16]. Since direct CP violation is predicted [3] and measured [11] to be small, $|\lambda|$ is set to 1.0.

2. Event selection

The data were collected with a trigger optimised for B hadrons having a J/ψ meson as a decay product. The trigger reconstructs a J/ψ meson from an oppositely charged muon pair using a set of selection criteria for muons and the J/ψ candidate. Both muons were required to have $p_T > 4$ GeV, $|\eta| < 2.2$ and cosine of the angle between the transverse decay length vector and the J/ψ momentum vector greater than 0.9. The muon pair is requested to have $p_T > 6.9$ GeV. The two muon tracks are fitted to a common decay vertex with a transverse decay length significance $L_{xy}/\sigma_{L_{xy}} > 3$, where L_{xy} is the distance between the beam spot and the secondary vertex in the transverse plane, and $\sigma_{L_{xy}}$ is its uncertainty. After the fit, the two muon tracks are required to have the distance of closest approach less than 5 mm. The J/ψ mass window is 2.9-3.3 GeV and the minimum vertex probability is 10 %.

After the trigger selection, the mass window for J/ψ is required to be within 150 MeV of the world average value of the J/ψ mass value. Transverse momentum of J/ψ candidate is required to be $p_T > 7$ GeV. Candidate $\phi(1020)$ mesons are reconstructed from pairs of oppositely charged tracks with $p_T > 0.7$ GeV. Each such a track is assumed to be a kaon and the invariant mass of a track pair is required to be within 10 MeV of the world average of $\phi(1020)$ mass.

The B_s candidates are formed subjecting the two muons and the two kaons to a combined vertex and kinematic fit, where the muon pair invariant mass is constrained to the world average of J/ψ mass. The B_s candidates with invariant mass between 5.2 GeV and 5.5 GeV and a χ^2 probability for the vertex fit greater than 2 % are selected.

Each event with a B_s candidate is required to have at least one reconstructed primary vertex. In case of several primary vertices, the one minimizing the angle between the B_s flight direction and transverse momentum vector is selected for B_s production vertex. This primary vertex is used to reconstruct the B_s proper decay length ct that is proper decay time t multiplied with velocity of light c. The proper decay length is defined as

$$ct = c\, m_{B_s} \frac{\vec{L}_{xy} \cdot \vec{p}_T}{p_T^2} \tag{2.1}$$

where m_{B_s} is the B_s mass set to the world best average, $\vec{L_{xy}}$ is the transverse decay length vector measured in the laboratory frame and $\vec{p_T}$ is the transverse momentum vector of the B_s meson.

3. Flavour tagging

The analysis uses electrons and muons originating from the decays of opposite-side B hadrons to define the initial flavour of the signal B_s meson. To separate correctly tagged leptons from mistagged ones, a selection is applied to electrons and muons. Tag muons are required to have $p_T > 2.2$ GeV and the 3D impact parameter d_{xyz} with respect to B_s primary vertex less than a millimeter. In addition, isolation ΔR between a B_s meson and a muon must be greater than 0.3. Electrons are required to have $p_T > 2.0$ GeV, $d_{xyz} < 1$ mm, $\Delta R > 0.2$ and a multivariate discriminator [17] improving the electron identification greater than 0.2.

After the initial selection of electrons and muons, a multilayer perceptron neural network (MLP-NN) of the TMVA toolkit [18] further improves the tagging. The training and the testing of muon and electron MLP-NN is done with more than 20 000 simulated $B_s \to J/\psi\phi$ events. As an input, neural networks use p_T, η, d_{xyz} of a lepton and two variables related to activity in a cone around lepton: a relative isolation variable and a p_T-weighted average of the charges of the particles in the cone. Additionally muon MLP-NN uses the p_T relative to the axis of the jet containing the muon and electron MLP-NN exploits the multivariate discriminator improving the electron identification.

Mistag probabilities are measured from data using $B^+ \to J/\psi K^+$ channel. The total tagging power obtained with this channel is $P_{tag} = (1.307 \pm 0.031\ (\text{stat}) \pm 0.007\ (\text{syst}))$ % and mistag probability $\omega = (30.17 \pm 0.24\ (\text{stat}) \pm 0.05\ (\text{syst}))$ %. The overall lepton tagging efficiency measured from data is (8.31 ± 0.03) %. Mistag probabilities are parametrised separately for electrons and muons as a function of the neural network output and the mistag probability is used in per-event fashion in the ϕ_s fit model.

4. Maximum likelihood fit

An unbinned extended maximum-likelihood fit to the data is performed using seven observables: B_s invariant mass, three decay angles Θ and flavour tag decision ξ, as well as proper decay length ct and its uncertainty σ_{ct}. The event likelihood function is given by

$$\begin{aligned} L &= N_{signal} \cdot L_{signal} + N_{background} \cdot L_{background} \\ L_{signal} &= \left(\tilde{f}(\Theta,\alpha,ct) \otimes G(ct,\sigma_{ct}) \cdot \varepsilon(\Theta)\right) \cdot P_S(m_{B_s}) \cdot P_S(\sigma_{ct}) \cdot P_S(\xi) \\ L_{background} &= P_{BG}(\cos\theta_T,\phi_T) \cdot P_{BG}(\cos\psi_T) \cdot P_{BG}(ct) \cdot P_{BG}(m_{B_s}) \cdot P_{BG}(\sigma_{ct}) \cdot P_{BG}(\xi) \end{aligned} \quad (4.1)$$

where L_{signal} is the probability distribution function (PDF) describing the $B_s \to J/\psi\phi$ signal component and $L_{background}$ is the PDF for the background model. Quantities N_{signal} and $N_{background}$ are the yields of signal and background events. The function $\tilde{f}(\Theta,\alpha,ct)$ is the modified differential decay rate $f(\Theta,\alpha,ct)$ of Eq. 1.1 containing the per-event tagging dilution term, $(1-2\omega)$. The phase δ_0 is set to zero, and the difference of phases $\delta_S - \delta_\perp$ is fit with one single parameter $\delta_{S\perp}$ to reduce the correlation among the various parameters.

The $\varepsilon(\Theta)$ is the angular efficiency and $G(ct, \sigma_{ct})$ is a Gaussian resolution function using the event-by-event proper decay length uncertainty σ_{ct}. $\Delta\Gamma_s$ is constrained to be positive [19]. The signal mass PDF $P_S(m_{B_s})$ is a sum of three Gaussian functions with a common mean. The background mass distribution is parametrised with an exponential function $P_{BG}(m_{B_s})$. The background decay length component $P_{BG}(ct)$ is a sum of two exponential functions. The angular background PDFs $P_{BG}(\cos\theta_T, \phi_T)$ and $P_{BG}(\cos\psi_T)$ are represented with a series of Legendre polynomials for $\cos\theta_T$ and $\cos\psi_T$ and sinusoidal functions are used to describe the angle φ_T. The decay length uncertainty functions $P_S(\sigma_{ct})$ and $P_{BG}(\sigma_{ct})$ are modelled with Gamma functions, two for the signal component and one for the background. The $P_S(\xi)$ and $P_{BG}(\xi)$ are the tag decision ξ PDFs obtained from the data.

5. Results and systematic uncertainties

The fit results with their statistical as well as the systematic uncertainties are given in Table 2 and the projections of the multidimensional fit are presented in Figure 1.

Magnitudes of different sources of systematic uncertainties for $\Delta\Gamma_s$ and ϕ_s are quantified by testing the assumptions made in the fit model and those associated to the fit procedure. The leading contribution of the systematic uncertainty of $\Delta\Gamma_s$ originates from proper decay length efficiency whereas ϕ_s has several equally large contributions of systematic uncertainty. The major contributions of systematic uncertainties for ϕ_s arise from modelling uncertainties of angular efficiencies, possible intrinsic bias of the fit model and setting the magnitude of the CP violation parameter $|\lambda|$ constant in the fit. Also the uncertainty related to the small mismatch of the modelling of the kaon p_T spectrum between data and simulated events has a contribution among the systematic uncertainties of ϕ_s.

The CMS result with the 68 % confidence-level contours and the results from ATLAS, CDF, D0 and LHCb experiments are presented in the $\Delta\Gamma_s$ - ϕ_s plane in Figure 2 [20]. The CMS result is in agreement with the standard model prediction and the results obtained from other experiments. The combined result is also consistent with the SM prediction.

	ϕ_s [rad]	$\Delta\Gamma_s$ [ps^{-1}]	$\lvert A_0\rvert^2$	$\lvert A_S\rvert^2$	$\lvert A_\perp\rvert^2$	$\delta_\parallel$ [rad]	$\delta_{S\perp}$ [rad]	$\delta_\perp$ [rad]	$c\tau$ [μm]
Fit result	-0.075 ± 0.097	0.095 ± 0.013	0.510 ± 0.005	$0.012^{+0.009}_{-0.007}$	0.243 ± 0.008	$3.48^{+0.07}_{-0.09}$	$0.37^{+0.28}_{-0.12}$	2.98 ± 0.36	447.2 ± 2.9
Source of syst. uncertainty									
PDL efficiency	0.002	0.0057	0.0015	-	0.0023	-	-	-	1.0
Angular efficiency	0.016	0.0021	0.0060	0.008	0.0104	0.674	0.14	0.66	0.8
Kaon p_T weighting	0.014	0.0015	0.0094	0.020	0.0041	0.085	0.11	0.02	1.1
PDL resolution	0.006	0.0021	0.0009	-	0.0008	0.004	-	0.02	2.9
Mistag distribution modelling	0.004	0.0003	0.0006	-	-	0.008	0.01	-	0.1
Flavour tagging	0.003	0.0003	-	-	-	0.006	0.02	-	-
Model bias	0.015	0.0012	0.0008	-	-	0.025	0.03	-	0.4
pdf modelling assumptions	0.006	0.0021	0.0016	0.002	0.0021	0.010	0.03	0.04	0.2
$\lvert\lambda\rvert$ as a free parameter	0.015	0.0003	0.0001	0.005	0.0001	0.002	0.01	0.03	-
Tracker alignment	-	-	-	-	-	-	-	-	1.5
Total systematic uncertainty	0.031	0.0070	0.0114	0.022	0.0116	0.680	0.18	0.66	3.7

Table 2: Summary of fit results and the systematic uncertainties of measured B_s parameters. If no value is given for a systematic uncertainty, this uncertainty is negligible compared to the statistical and other systematic uncertainties. The total systematic uncertainty is the quadratic sum of the listed systematic uncertainties.

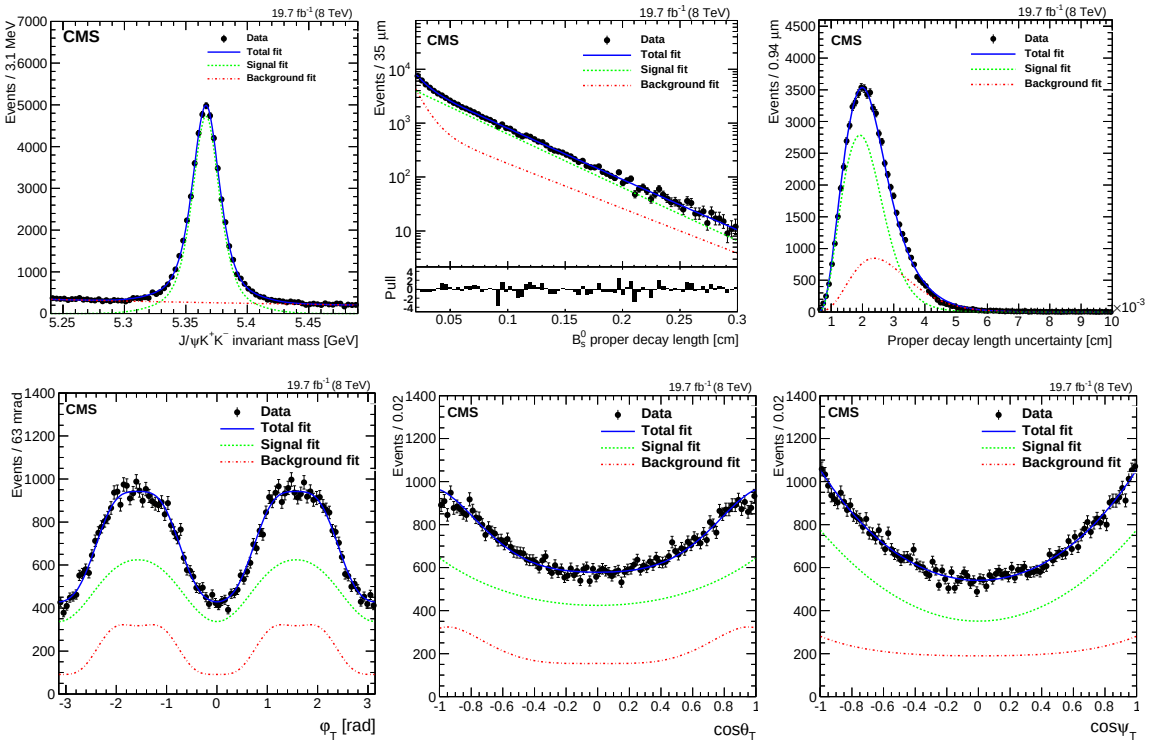

Figure 1: Fit projections to the six observables including B_s mass, proper decay length ct and its uncertainty and the three angular distributions $\phi_T, \cos\theta_T$ and $\cos\psi_T$.

6. Summary and outlook

The CMS experiment measured the weak mixing phase ϕ_s and the decay width difference $\Delta\Gamma_s$ between the B_s mass eigenstates using pp collision data having centre-of-mass energy of 8 TeV and integrated luminosity of 19.7 fb^{-1}. The measurement is done with 49 200 $B_s \to J/\psi\phi$ signal candidates extracted from pp data. The analysis utilises opposite-side electron and muon tagging to identify the B_s flavour at the production time of the meson. The measured values for the weak phase and the decay width difference are $\phi_s = -0.075 \pm 0.097\ (\text{stat}) \pm 0.031\ (\text{syst})$ rad and $\Delta\Gamma_s = 0.095 \pm 0.013\ (\text{stat}) \pm 0.007\ (\text{syst})$ ps^{-1}. The measured values of ϕ_s and $\Delta\Gamma_s$ are in agreement with the standard model predictions and the result confirms $\Delta\Gamma_s$ to be nonzero. Our analysis provides a reference measurement of ϕ_s and $\Delta\Gamma_s$ and has a contribution to improving the overall precision of these quantities. Because the precision of our measurement is dominated by statistical uncertainty, the goal for run II of the LHC is to reduce the statistical error by performing the analysis with a larger dataset having a center-of-mass energy of 13 TeV.

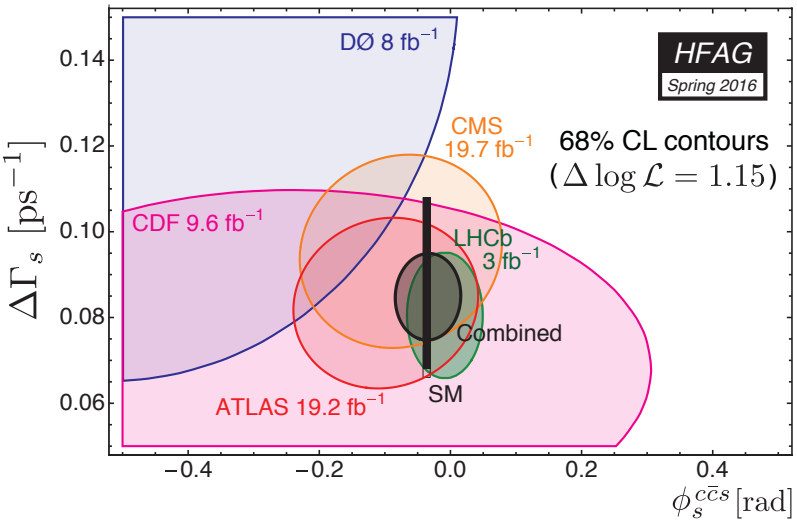

Figure 2: The individual 68 % confidence-level contours of ATLAS, CMS, CDF, D0 and LHCb results in $\Delta\Gamma_s$ - ϕ_s plane, their combined contour denoted as solid line and shaded area, and the standard model predictions for $\Delta\Gamma_s$ and ϕ_s marked as thin black rectangle [20].

References

[1] CMS Collaboration, *Measurement of the CP-violating weak phase* ϕ_s *and the decay width difference* $\Delta\Gamma_s$ *using the* $B_s^0 \to J/\psi\phi(1020)$ *decay channel in pp collisions at* $\sqrt{s} = 8$ *TeV*, Phys. Lett. B 757 (2016) 97, doi:10.1016/j.physletb.2016.03.046, arXiv:1507.07527.

[2] CMS Collaboration, *The CMS experiment at the CERN LHC*, JINST 3 S08004 (2008).

[3] J. Charles et al, *Predictions of selected flavour observables within the standard model*, Phys. Rev. D 84 (2011) 033005, doi:10.1103/PhysRevD.84.033005, arXiv:1106.4041.

[4] A. Lenz and U. Nierste *Numerical updates of lifetimes and mixing parameters of B mesons*, in Proceedings of the 6th International Workshop on the CKM Unitarity Triangle, T. Gershon, ed. University of Warwick, United Kingdom, September, 2010.

[5] CDF Collaboration, *First flavor-tagged determination of bounds on mixing-induced CP Violation in* $B_s \to J/\psi\phi$ *decays*, Phys. Rev. Lett. 100 (2008) 161802, doi:10.1103/PhysRevLett.100.161802, arXiv:0712.2397.

[6] D0 Collaboration, *Measurement of* B_s *mixing parameters from the flavor-tagged decay* $B_s \to J/\psi\phi$, Phys. Rev. Lett. 101 (2008) 241801, doi:10.1103/PhysRevLett.101.241801, arXiv:0802.2255.

[7] CDF Collaboration, *Measurement of the CP-violating phase* β_s *with the CDF II detector*, Phys. Rev. D 85 (2012) 072002, doi:10.1103/PhysRevD.85.072002, arXiv:1112.1726.

[8] CDF Collaboration, *Measurement of the CP-violating phase* ϕ_s *using the flavor-tagged decay* $B_s \to J/\psi\phi$ *in* $8\,fb^{-1}$ $p\bar{p}$ *collisions* ,Phys. Rev. D 85 (2012) 032006, doi:10.1103/PhysRevD.85.032006, arXiv:1109.3166.

[9] LHCb Collaboration, *Measurement of the CP-violating phase* ϕ_s *in* $\overline{B}_s^0 \to J/\psi\pi^+\pi^-$ *decays*, Phys. Lett. B 736 (2014), doi:10.1016/j.physletb.2014.06.079, arXiv:1405.4140.

[10] LHCb Collaboration, *Measurement of CP violation and the B_s^0 meson decay width difference with $B_s^0 \to J/\psi K^+K^-$ and $B_s^0 \to J/\psi\pi^+\pi^-$ decays*, Phys.Rev. D 87 (2013), doi:10.1103/PhysRevD.87.112010, arXiv:1304.2600.

[11] LHCb Collaboration, *Measurement of the CP-violating phase ϕ_s in $\overline{B}_s^0 \to J/\psi\pi^+\pi^-$ decays*, Phys. Lett. B 713 (2012), doi:10.1016/j.physletb.2012.06.032, arXiv:1204.5675.

[12] ATLAS Collaboration, *Time-dependent angular analysis of the decay $B_s^0 \to J/\psi\phi$ and extraction of $\Delta\Gamma_s$ and the CP-violating weak phase ϕ_s by ATLAS*, JHEP 1212 072 (2012), doi:10.1007/JHEP12(2012)072, arXiv:1208.0572.

[13] ATLAS Collaboration, *Flavour tagged time dependent angular analysis of the $B_s \to J/\psi\phi$ decay and extraction of $\Delta\Gamma$ and the weak phase ϕ_s in ATLAS*, Phys. Rev. D 90, 052007 (2014), doi:10.1103/PhysRevD.90.052007, arXiv:1407.1796.

[14] ATLAS Collaboration, *Measurement of the CP-violating phase ϕ_s and B_s^0 meson decay width difference with $B_s^0 \to J/\psi\phi$ decays at ATLAS*, Submitted to JHEP, arXiv:1601.03297.

[15] A. S. Dighe et al, *Angular distributions and lifetime differences in $B_s^0 \to J/\psi\phi$ decays*, Phys. Lett. B 369 (1996) 144, doi:10.1016/0370-2693(95)01523-X, arXiv:hep-ph/9511363.

[16] G.C Branco, L. Lavoura and J.P. Silva *CP violation*, Int. Ser. Monogr. Phys. 103 (1999) 1.

[17] CMS Collaboration, *Commissioning of the Particle-flow Event Reconstruction with the first LHC collisions recorded in the CMS detector*, CMS Physics Analysis Summary CMS-PAS-PFT-10-001, 2010.

[18] A. Hoecker et al, *TMVA: Toolkit for multivariate data analysis*, PoS ACAT 2007 040, arXiv:physics/0703039.

[19] LHCb Collaboration, *Determination of the sign of the decay width difference in the B_s^0 system*, Phys. Rev. Lett. 108 (2012) 241801, doi:10.1103/PhysRevLett.108.241801, arXiv:1202.4717.

[20] Y. Amhis et al. (Heavy Flavour Averaging Group), *Averages of b-hadron, c-hadron, and τ-lepton properties as of summer 2014*, arXiv:1412.7515.